

References

Afolabi, D. (1988). *Modal characteristics of turbomachine blades in a multi-stage engine*. Proceedings of the 6th International Modal Analysis Conference: Orlando, Florida, 521-527.

Al-Bedoor, B.O. (2002). Blade vibration measurement in turbo-machinery: Current status. *Shock and Vibration Digest*, 34(6), 455-461.

Antoni, J., Randall, R.B. (2004a). Unsupervised noise cancellation for vibration signals: Part I - Evaluation of adaptive algorithms. *Mechanical Systems and Signal Processing*, 18(1), 89-101.

Antoni, J., Randall, R.B. (2004b). Unsupervised noise cancellation for vibration signals: Part II - A novel frequency-domain algorithm. *Mechanical Systems and Signal Processing*, 18(1), 103-117.

Aono, H., Chikata, T., Hagiwara, Y., Inuma, H. (1985). *Optical fan blade vibration measurement*. International Congress on Experimental Mechanics: Beijing, China, 571-576.

Aretakis, N., Mathioudakis, K., Dedoussis, V. (1998). Derivation of signatures for faults in gas turbine compressor blading. *Control Engineering Practice*, 6, 969-974.

Balda, M. (2000). *Processing of blade monitoring system data*. Proceedings of the 7th International Conference on Vibrations in Rotating Machinery: Nottingham, UK, 677-685.

Balmès, E. (1997). *Structural Dynamics Toolbox user's guide*. France: Scientific Software.

Beaumont, R. (21 October 2004). Personal communication.

Beuseroy, P., Lengellé, R. (2007). Nonintrusive turbomachine blade vibration measurement system. *Mechanical Systems and Signal Processing*, 21(4), 1717-1738.

Bell, J.R., Rothberg, S.J. (2000). Laser vibrometers and contacting transducers, target rotation and six degree-of-freedom vibration: What do we really measure? *Journal of Sound and Vibration*, 237(2), 245-261.

Bhat, M.M., Ramamurti, V., Sujatha, C. (1996). Studies on the determination of natural frequencies of industrial turbine blades. *Journal of Sound and Vibration*, 196(5), 570-692.

Boutarek, N., Saïdi, D., Acheheb, M.A., Iggui, M., Bouterfaïa, S. (2008). Competition between three damaging mechanisms in the fractured surface of an Inconel 713 superalloy. *Materials Characterization*, 59(7), 951-956.

Brincker, R, Andersen, P., Martinez, M.E., Tallavó, F. (1996). *Modal analysis of an offshore platform using two different ARMA approaches*. Proceedings of the 14th International Modal Analysis Conference: Detroit, Michigan, 1197-1203.

Caponero, M.A., Pasqua, P., Paolozzi, A., Peroni, I. (2000). Use of Holographic interferometry and electronic speckle pattern interferometry for measurements of dynamic displacements. *Mechanical Systems and Signal Processing*, 14(1), 49-62.

Castellini, P., Santolini, C. (1998). Vibration measurements on blades of a naval propeller rotating in water with tracking laser vibrometer. *Measurement*, 24, 43-54.

Cauberghe, B., Guillaume, P., Verboven, P., Parloo, E. (2003). Identification of modal parameters including unmeasured forces and transient effects. *Journal of Sound and Vibration*, 265, 609-625.

Chuckpaiwong, I. (2003). *Development of position sensor using phase-based continuous wave radar*. D.Phil. Thesis. Atlanta: Georgia Institute of Technology.

Cookson, R.A., Bandyopahyay, P. (1980). A fiber-optic laser-Doppler probe for vibration analysis of rotating machines. *Transactions of the ASME: Journal of Engineering for Power*, 102, 607-612.

Davis, Q.V., Kulczyk, K.W. (1969). Vibrations of turbine blades measured by means of a laser. *Nature*, 222, 475-476.

Denman, M., Halliwell, N., Rothberg, S. (1996). *Speckle noise reduction in laser vibrometry: Experimental and numerical optimization*. Proceedings of SPIE: The International Society for Optical Engineering, 2868: Ancona, Italy, 12-21.

Drumm, M., Haase, W.C. (2000). *High performance rotor health monitoring*. Proceedings of the 19th Digital Avionics Systems Conference, 2: Philadelphia, PA, 6E4/1-6E4/8.

Ellis, R., Gulick, D. (1994). *Calculus with analytical geometry*. 5th edition. Florida: Saunders College Publishing.

Ewald, D., Pavlovic, A., Bollinger, J.G. (1971). Noise reduction by applying modulation principles. *The Journal of the Acoustical Society of America*, 49(5A), 1381-1385.

Ewins, D.J. (2000). *Modal testing theory, practice and application*. 2nd edition. Baldock: Research Studies Press.

Fan, Y.C., Ju, M.S., Tsuei, Y.G. (1994). Experimental study on vibration of a rotating blade. *Journal of Engineering for Gas Turbines and Power*, 116, 672-677.

Fangman, C.N., Zastrow, V.A., Bobeck, J.E. (1967). High-speed-turbocharger blade-vibration measurement. *Experimental Mechanics*, 7(1), 19A-21A.

Fante, R.L. (1988). *Signal analysis and estimation: An introduction*. New York: Wiley.

Finke, C., Schmidt, R. (1996). Effizientes Lasermessverfahren zur untersuchung von schaufelschwingungen [Laser technique for efficient blade vibration measurements]. *VDI Berichte*, 1249, 125-138.

Gadala, M.S., Byrne, T.P. (1986). *Modelling of turbine blades for stress and dynamic analysis*. Proceedings of the 4th International Modal Analysis Conference: Los Angeles, CA, 1220-1227.

Gamba, J., Shimamura, T. (2005). Spectrum estimation by noise-compensated data extrapolation. *IEICE Transactions on Fundamentals of Electronics, Communications and Computer Sciences*, E88(3), 702-710.

Giordano, A.A., Hsu, F.M. (1985). *Least square estimation with applications to digital signal processing*. New York: Wiley.

Gloger (1988). *Kendal T 7353 Special Measurements during commissioning*. (WT TVL/88/018). Mülheim: Siemens AG KWU Group.

Halkon, B.J., Rothberg, S.J. (2006). Vibration measurements using continuous scanning laser vibrometry: Advanced aspects in rotor applications. *Mechanical Systems and Signal Processing*, 20(6), 1286-1299.

Halliwell, N.A. (1996). The laser torsional vibrometer: A step forward in rotating machinery diagnostics. *Journal of Sound and Vibration*, 190(3), 399-418.

Hay, A.M. (2002). Dynamic-Q algorithm for constrained optimization: General mathematical programming code (Computer software). Pretoria: University of Pretoria.

Heath, S., Imregun, M. (1998). A survey of blade tip-timing measurement techniques for turbomachinery vibration. *Journal of Engineering for Gas Turbines and Power*, 120(4), 784-791.

Hirata, Y. (2005). Non-harmonic Fourier analysis available for detecting very low-frequency components. *Journal of Sound and Vibration*, 287(3), 611-613.

Hollkamp, J.J., Gordon, R.W. (2001). Modal test experiences with a jet engine fan model. *Journal of Sound and Vibration*, 248(1), 151-165.

Holst, T.A. (2005). *Analysis of spatial filtering in phase-based microwave measurements of turbine blade tips*. Master's Thesis. Atlanta: Georgia Institute of Technology.

Hueck, U. (19 March 2004). Personal communication.

Hwang, Y., Lee, I., Lee, J.M., Lee, S.B. (2006). *A new online rotor condition monitoring method using FBG sensors and no telemetry system*. Proceedings of the 13th International Congress on Sound and Vibration: Vienna, Austria, 390-397.

Imregun, M., Visser, W.J. (1991). A review of model updating techniques. *The Shock and Vibration Digest*, 23, 9-20.

Imregun, M., Visser, W.J., Ewins, D.J. (1995). Finite element model updating using frequency response function data: I. Theory and initial investigation. *Mechanical Systems and Signal Processing*, 9(2), 187-202.

Infante, V., Silva, J.M., de Freitas, M., Reis, L. (2009). Failures analysis of compressor blades of aeroengines due to service, *Engineering Failure Analysis*, 16(4), 1118-1125.

Irrerier, H. (1988). Free and forced vibrations of turbine blades. In *Rotordynamics 2: Problems in turbomachinery*. Edited by Rieger, N.F. Italy: International Centre for Mechanical Sciences, 397-422.

Jacobs, G.B., Grady, G. (1977). Turbine blade vibration sensor. *IEEE Journal of Quantum Electronics*, 13(9), 827-828.

Jacobs, S., De Roeck, G. (2003). *Dynamic testing of a pre-stressed concrete beam*. Proceedings of the 6th National Congress on Theoretical and Applied Mechanics: Ghent, Belgium.

Kadoya, Y., Mase, M., Kaneko, Y., Umemura, S., Oda, T., Johnson, M.C. (1995). Noncontact vibrational measurement technology of steam turbine blade. *JSME International Journal, Series C*, 38(3), 486-493.

Kielb, J.J., Abhari, R.S. (2003). Experimental study of aerodynamic and structural damping in a full-scale rotating turbine. *Journal of Engineering for Gas Turbines and Power*, 125(1), 102-112.

King, S., Anuzis, P., King, D., Tarassenko, L., Utete, S., McGrogan, N. (2006). *A review of applications for advanced engine health monitoring in civil aircraft engines*. Proceedings of the 13th International Congress on Sound and Vibration: Vienna, Austria, 15-22.

Kulczyk, W.K., Davis, Q.V. (1970). Laser measurements of vibrations on rotating objects. *Opto-Electronics*, 2, 177-179.

Kulczyk, W.K., Davis, Q.V. (1973). Laser Doppler instrument for measurement of vibration of moving turbine blades. *Proceedings of the Institute of Electrical Engineers*, 120(9), 1017-1023.

Kumar, S., Roy, N., Ganguli, R. (2007). Monitoring low cycle fatigue damage in turbine blade using vibration characteristics. *Mechanical Systems and Signal Processing*, 21(1), 480-501.

Leissa, A.W. (1969). *Vibration of plates* (SP-160), Washington: NASA.

Lesne, J.L., Fevrier, T., Triquigneaux, P., Le Floc'h, C. (1985). *Vibratory analysis of a rotating bladed disk using holographic interferometry and laser vibrometry*. Proceedings of SPIE - The International Society for Optical Engineering, 599, Cannes, France, 74-79.

Lobos, T., Leonowicz, Z., Rezmer, J., Schegner, P. (2006). High-resolution spectrum-estimation methods for signal analysis in power systems. *IEEE Transactions on Instrumentation and Measurement*, 55(1), 219-225.

Lv, J., Wang, J., Chen, D. (2003). *Experimental studies for micro helicopter blade dynamics*. 5th International Symposium on Test and Measurement: Shenzhen, China, 33-36.

Mansidor, M.R. (2002). *Resonant blade response in turbine rotor spin tests using a laser-light probe non-intrusive measurement system*. Master's Thesis. California: Naval Postgraduate School.

Marple, S.L. (1987). *Digital spectral analysis with applications*. New Jersey: Prentice-Hall.

Martarelli, M., Ewins, D.J. (2006). Continuous scanning laser Doppler vibrometry and speckle noise occurrence. *Mechanical Systems and Signal Processing*, 20(8), 2277-2289.

Mathwin, K. (March 2004). Personal communication.

Maynard, K., Trethewey, M., Gill, R., Resor, B. (2001). *Gas turbine blade and disk crack detection using torsional vibration monitoring: A feasibility study*. Proceedings

of 14th International Congress on Condition Monitoring and Diagnostic Engineering Management: Manchester, UK.

Mazur, Z., Garcia-Illescas, R., Aguirre-Romano, J., Perez-Rodriguez, N. (2008). Steam turbine blade failure analysis. *Engineering Failure Analysis*, 15(1-2), 129-141.

Mazur, Z., Hernández-Rossette, A., García-Illescas, R. (2006). Investigation of the failure of the L-0 blades. *Engineering Failure Analysis*, 13(8), 1338-1350.

Muraoka, T., Nishioka, Y. (2004). *Separation of adjacent frequency components in Generalized Harmonic Analysis (GHA)*. Proceedings of the 46th IEEE International Midwest Symposium on Circuits and Systems, 2: Hiroshima, Japan, II157-II160.

Newby, M. (21 October 2004). Personal communication.

Nikolic, M., Petrov, E.P., Ewins, D.J. (2007). Coriolis forces in forced response analysis of mistuned bladed disks. *Journal of Turbomachinery*, 129(4), 730-739.

Norton, M.P., Karczub, D.G. (2003). *Fundamentals of noise and vibration analysis for engineers*. 2nd edition. Cambridge: Cambridge University Press.

Oberholster, A.J., Heyns, P.S. (2006). On-line fan blade damage detection using neural networks. *Mechanical Systems and Signal Processing*, 20(1), 78-93.

Oberholster, A.J., Heyns, P.S. (2008). *A study of the non-harmonic Fourier analysis technique*. Proceedings of the 21st International Congress on Condition Monitoring and Diagnostic Engineering Management: Prague, Czech Republic, 361-370.

Oberholster, A.J., Heyns, P.S. (2009). Online condition monitoring of axial-flow turbomachinery blades using rotor-axial Eulerian laser Doppler vibrometry. *Mechanical Systems and Signal Processing*, 23(5), 1634-1643.

Oberholster, A.J., Heyns, P.S. (In press). Eulerian laser Doppler vibrometry: Online blade damage identification on a multi-blade test rotor. *Mechanical Systems and Signal Processing*. (DOI 10.1016/j.ymssp.2010.03.007).

Orsagh, R.F., Roemer, M.J. (2002). *Examination of successful modal analysis techniques used for bladed-disk assemblies*. Proceedings of the 56th Conference Of

The Society For Machinery Failure Prevention Technology: Virginia Beach, VA, 495-506.

Pfister, T., Buttner, L., Czarske, J., Krain, H., Schodl, R. (2006). Turbo machine tip clearance and vibration measurements using a fibre optic laser Doppler position sensor. *Measurement Science and Technology*, 17(7), 1693-1705.

Pruemont, A. (2002). *Vibration control of active structures: An introduction*. 2nd edition. Belgium: Kluwer Academic Publishers.

Rao, J.S., Sreenivas, R. (2003). *Dynamics of asymmetric rotors using solid models*. Proceedings of the International Gas Turbine Congress: Tokyo, Japan, TS-016.

Rao, J.S., Vyas, N.S. (1985). *Response of steam turbine blades subjected to distributed harmonic nozzle excitation*. Proceedings of the 3rd International Modal Analysis Conference: Orlando, Florida, 618-626.

Rao, S.S. (1995). *Mechanical vibrations*. 3rd edition. New York: Addison-Wesley Publishing Company.

Reinhardt, A.K., Kadambi, J.R., Quinn, R.D. (1995). Laser vibrometry measurements of rotating blade vibrations. *Transactions of the ASME: Journal of Engineering for Gas Turbines and Power*, 117(3), 484-488.

Rieger, N.F. (1988). The diagnosis and correction of steam turbine blade problems. In *Rotordynamics 2: Problems in turbomachinery*. Edited by Rieger, N.F. Italy: International Centre for Mechanical Sciences, 453-483.

Rothberg, S. (2006). Numerical simulation of speckle noise in laser vibrometry. *Applied Optics*, 45(19), 4523-4533.

Rothberg, S.J., Baker, J.R., Halliwell, N.A. (1989). Laser vibrometry: Pseudo-vibrations. *Journal of Sound and Vibration*, 135(3), 516-522.

Schwingshackl, C., Massei, L., Zang, C., Ewins, D. (2010). A constant scanning LDV technique for cylindrical structures: Simulation and measurement. *Mechanical Systems and Signal Processing*, 24(2), 394-405.

Sever, I.A. (2004). *Experimental validation of turbomachinery blade vibration predictions*. D.Phil. Thesis. London: University of London.

Shen, F., Zheng, M., Feng Shi, D., Xu, F. (2003). Using the cross-correlation technique to extract modal parameters on response-only data. *Journal of Sound and Vibration*, 259(5), 1163-1179.

Simani, S. (2005). Identification and fault diagnosis of a simulated model of an industrial gas turbine. *IEEE Transactions on Industrial Informatics*, 1(3), 202-216.

Singh, M.P. (1998). Probabilistic estimation of the effect of dimensional tolerance for turbine/compressor blade attachment. *American Society of Mechanical Engineers: Pressure Vessels and Piping Division*, 381, 247-251.

Spicer, D. (03 April 2003a). Draft report on Duvha explosion next week. *Engineering News*, n.p.

Spicer, D. (18 April 2003b). Duvha set for refurb after explosion. *Engineering News*, n.p.

Sreenivasamurthy, S., Ramamurti, V. (1981). Coriolis effect on the vibration of flat rotating low aspect ratio cantilever plates. *Journal of Strain Analysis*, 16(2), 97-106.

Sriram, P., Hanagud, S., Craig, J.I. (1992). Mode shape measurement using a scanning laser Doppler vibrometer. *International Journal of Analytical and Experimental Modal Analysis*, 7(3), 169-178.

Stanbridge, A.B., Ewins, D.J. (1996). *Using a continuously-scanning laser Doppler vibrometer for modal testing*. Proceedings of the 14th International Modal Analysis Conference: Detroit, Michigan, 816-822.

Stanbridge, A.B., Ewins, D.J. (1999). Modal testing using a scanning laser Doppler vibrometer. *Mechanical Systems and Signal Processing*, 13(2), 225-270.

Steele, K.E. (1999). Ocean wave heave time series as the sum of nonharmonic signals. *Ocean Engineering*, 26(12), 1335-1357.

Tappert, P., Von Flotow, A., Mercadal, M. (2001). Autonomous PHM with blade-tip sensors: Algorithms and seeded fault experience. *IEEE Proceedings of the Aerospace Conference*, 7, 3287-3295.

The Mathworks. (2006). *Signal Processing Toolbox for use with Matlab: User's guide*. Natick: The Mathworks, Inc.

Truman, J.C., Martin, J.R., Klint, R.V. (1961). Pulsed-air vibration technique for testing high-performance turbomachinery blading. *Experimental Mechanics*, 1(6), 201-205.

Vanlanduit, S., Daerden, F., Guillaume, P. (2007). Experimental modal testing using pressurized air excitation. *Journal of Sound and Vibration*, 299(1-2), 83-98.

Visser, J. (20 September 2004). Personal communication.

Von Flotow, A., Mercadal, M., Tappert, P. (2000). Health monitoring and prognostics of blades and disks with blade tip sensors. *IEEE Aerospace Conference Proceedings*, 6, 433-440.

Watkins, W.B., Chi, R.M. (1989). Noninterference blade-vibration measurement system for gas turbines. *Journal of Propulsion and Power*, 5(6), 727-730.

White, F.M. (1999). *Fluid mechanics*. 4th edition. Singapore: McGraw-Hill.

Wilmshurst, T.H., Halliwell, N.A. (1993). Laser vibrometer speckle-noise cancellation. *Measurement Science and Technology*, 4(4), 479-487.

Wu, M.C., Huang, S.C. (1998). On the vibration of a cracked rotating blade. *Shock and Vibration*, 5(5), 317-323.

Yang, K., Cho, C., Bae, C., Kim, G., Lee, W., Song, O. (2006). Study on changes of dynamic characteristics according to cracked condition in a turbine blade. Proceedings of the 13th International Congress on Sound and Vibration, 468-475.

Ziegler, H. (1994). Measuring turbine blade vibration. *ABB Review*, 1(9), 31-34.

References



Zielinski, M., Ziller, G. (2000). Noncontact vibration measurements on compressor rotor blades. *Measurement Science and Technology*, 11(7), 847-856.

Appendix A Rotor-Circumferential ELDV

A.1 Introduction

Whereas rotor-axial ELDV provides information on mainly the flap-wise on torsional vibration behaviour of the blade, the question arises whether any useful information is available from sideways vibration behaviour. To investigate this, it is necessary to align the LDV to measure along the blade leading edge in the plane of rotation as given in Figure 74 for a single-blade rotor. This will henceforth be referred to as Rotor-Circumferential (RC) ELDV. Jacobs and Grady (1977) present a system that allows RC TLDV using a scanning mirror directing the laser beam on a parabolic mirror. However no literature could be found on RC ELDV.

Evaluating Figure 74, it is clear that the circumferential speed of the blade will affect the measurements. Also the incidence angle of the laser beam relative to the blade edge normal will change continuously. Furthermore it is important to establish whether the ELDV scanning speed remains constant over the blade leading edge at a constant rotation speed. To address these issues, it is necessary to employ vector-loop calculations.

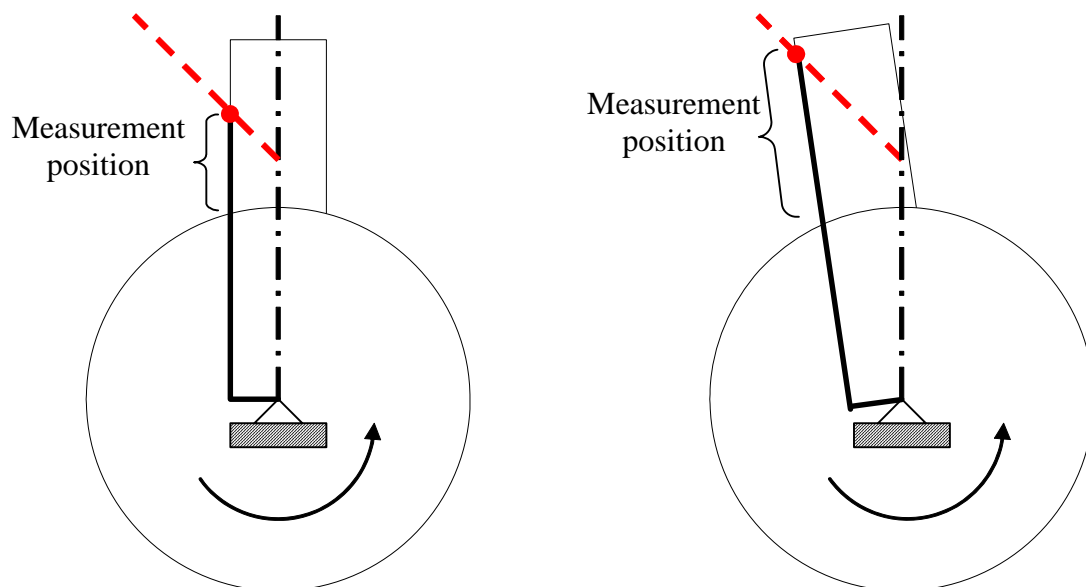


Figure 74: Effect of blade rotation on LDV measurement position

A.2 RC ELDV mathematical definition

A.2.1 Vector-loop equations

An equivalent mechanical system of the RC ELDV measurement technique is shown in Figure 75 along with its corresponding vector-loop diagram and the coordinate system used. It is important to define here the Mean Blade Leading Edge Curve (MBLEC). The MBLEC is obtained by drawing a straight line through the mean of the actual Blade Leading Edge Profile (BLEP) as demonstrated in Figure 76 for an arbitrary BLEP.

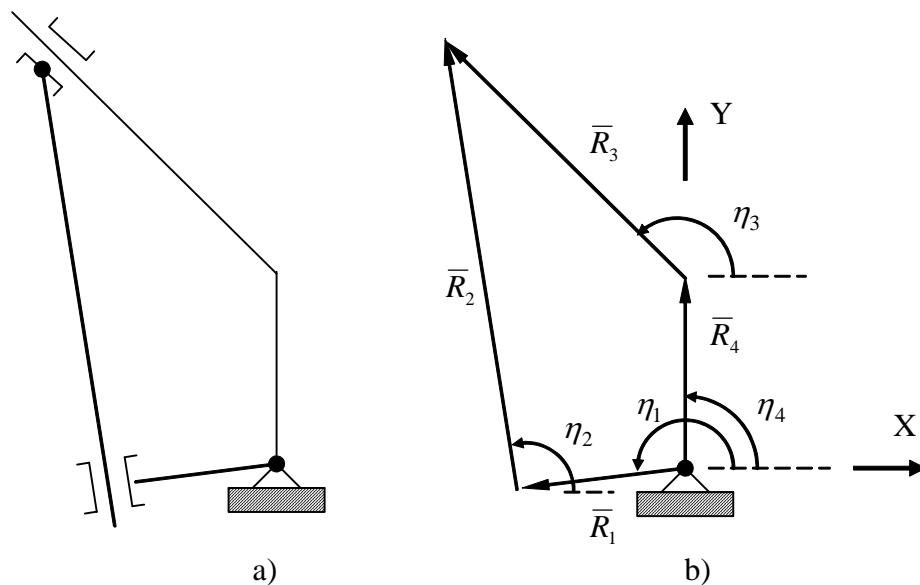


Figure 75: a) Equivalent mechanical system b) Vector-loop diagram

The vector notation used given by Equation 47:

$$\bar{R}_h = |\bar{R}_h| e^{i\angle \bar{R}_h} = R_h e^{i\eta_h}$$

Equation 47

with h the vector number.

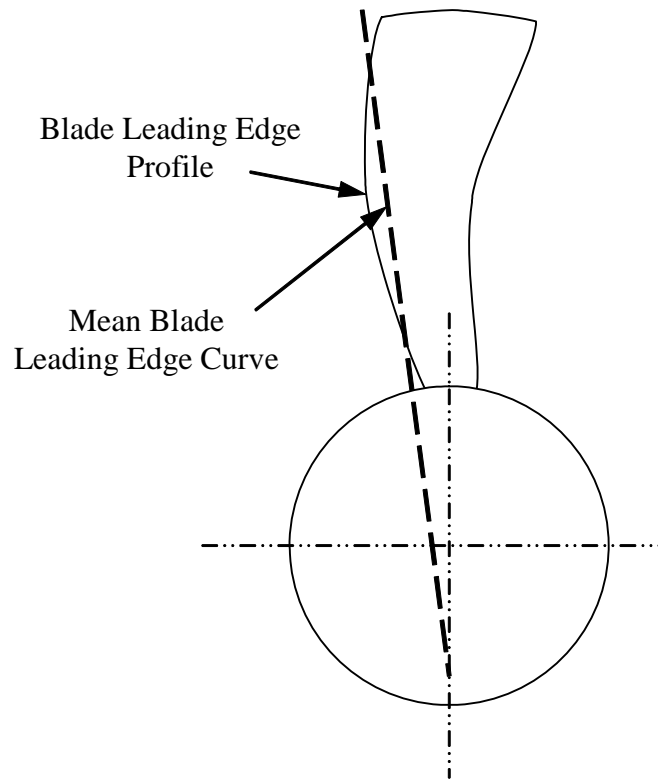


Figure 76: Mean Blade Leading Edge Curve

The four vectors shown in Figure 75 can be defined as follows:

1. \bar{R}_1 describes the MBLEC offset. It starts from the rotation axis and terminates at its intersection to the MBLEC, perpendicular to that curve. This results in

$$\eta_2 = \eta_1 - 90^\circ$$

Equation 48

which leads to the trigonometric relationships

$$\begin{aligned} \cos \eta_2 &= \sin \eta_1 \\ \text{and } \sin \eta_2 &= -\cos \eta_1 \end{aligned}$$

Equation 49

2. \bar{R}_2 defines the instantaneous measurement position of the laser beam on the MBLEC.
3. \bar{R}_3 gives the laser orientation and reaches from the laser beam intersection with the ZY plane to the measurement point location, which is at the end of \bar{R}_2 .
4. \bar{R}_4 is defined as the laser offset vector, starting from the rotation axis along the ZY plane to the start of \bar{R}_3 .

Along with the vector definitions, the following assumptions are made:

1. RC blade vibration is ignored along with any motion of the centre of rotation of the shaft from the coordinate system origin. This means that \bar{R}_1 and \bar{R}_2 remain perpendicular and that \bar{R}_4 and R_1 are constant.
2. The LDV is furthermore assumed to be perfectly stationary. As a result, η_3 is constant as well.

Using the vector-loop method, Equation 50 is obtained:

$$\begin{aligned}\bar{R}_1 + \bar{R}_2 - \bar{R}_3 - \bar{R}_4 &= 0 \\ R_1 e^{i\eta_1} + R_2 e^{i\eta_2} - R_3 e^{i\eta_3} - R_4 e^{i\eta_4} &= 0\end{aligned}$$

Equation 50

Rearranging for the real part of Equation 50:

$$\begin{aligned}R_1 \cos \eta_1 + R_2 \cos \eta_2 - R_3 \cos \eta_3 - R_4 \cos \eta_4 &= 0 \\ R_1 \cos \eta_1 + R_2 \sin \eta_1 - R_3 \cos \eta_3 &= 0 \\ R_2 \sin \eta_1 - R_3 \cos \eta_3 &= -R_1 \cos \eta_1\end{aligned}$$

Equation 51

Rearranging for the imaginary part of Equation 50:

$$\begin{aligned}R_1 \sin \eta_1 + R_2 \sin \eta_2 - R_3 \sin \eta_3 - R_4 \sin \eta_4 &= 0 \\ R_1 \sin \eta_1 - R_2 \cos \eta_1 - R_3 \sin \eta_3 - R_4 &= 0 \\ -R_2 \cos \eta_1 - R_3 \sin \eta_3 &= R_4 - R_1 \sin \eta_1\end{aligned}$$

Equation 52

To calculate velocities, Equation 50 is differentiated with respect to time:

$$\begin{aligned}\frac{d}{dt} (R_1 e^{i\eta_1} + R_2 e^{i\eta_2} - R_3 e^{i\eta_3} - R_4 e^{i\eta_4}) &= 0 \\ i\dot{\eta}_1 R_1 e^{i\eta_1} + i\dot{\eta}_2 R_2 e^{i\eta_2} + \dot{R}_2 e^{i\eta_2} - \dot{R}_3 e^{i\eta_3} &= 0 \\ i\dot{\eta}_1 R_1 (\cos \eta_1 + i \sin \eta_1) + i\dot{\eta}_2 R_2 (\cos \eta_2 + i \sin \eta_2) + \dot{R}_2 (\cos \eta_2 + i \sin \eta_2) - \dot{R}_3 (\cos \eta_3 + i \sin \eta_3) &= 0\end{aligned}$$

Equation 53

The real part of Equation 53 can be rearranged as:

$$\begin{aligned}-R_1 \dot{\eta}_1 \sin \eta_1 - R_2 \dot{\eta}_2 \sin \eta_2 + \dot{R}_2 \cos \eta_2 - \dot{R}_3 \cos \eta_3 &= 0 \\ -R_1 \dot{\eta}_1 \sin \eta_1 + R_2 \dot{\eta}_1 \cos \eta_1 + \dot{R}_2 \sin \eta_1 - \dot{R}_3 \cos \eta_3 &= 0 \\ R_2 \dot{\eta}_1 \cos \eta_1 + \dot{R}_2 \sin \eta_1 - \dot{R}_3 \cos \eta_3 &= R_1 \dot{\eta}_1 \sin \eta_1\end{aligned}$$

Equation 54

While the imaginary part Equation 53 is rearranged as:

$$\begin{aligned}
 R_1 \dot{\eta}_1 \cos \eta_1 + R_2 \dot{\eta}_2 \cos \eta_2 + \dot{R}_2 \sin \eta_2 - \dot{R}_3 \sin \eta_3 &= 0 \\
 R_1 \dot{\eta}_1 \cos \eta_1 + R_2 \dot{\eta}_1 \sin \eta_1 - \dot{R}_2 \cos \eta_1 - \dot{R}_3 \sin \eta_3 &= 0 \\
 R_2 \dot{\eta}_1 \sin \eta_1 - \dot{R}_2 \cos \eta_1 - \dot{R}_3 \sin \eta_3 &= -R_1 \dot{\eta}_1 \cos \eta_1
 \end{aligned}$$

Equation 55

Combing Equation 51, Equation 52, Equation 54 and Equation 55 in matrix form:

$$\begin{bmatrix} \sin \eta_1 & -\cos \eta_3 & 0 & 0 \\ -\cos \eta_1 & -\sin \eta_3 & 0 & 0 \\ \dot{\eta}_1 \cos \theta_1 & 0 & \sin \eta_1 & -\cos \eta_3 \\ \dot{\eta}_1 \sin \theta_1 & 0 & -\cos \eta_1 & -\sin \eta_3 \end{bmatrix} \begin{bmatrix} R_2 \\ R_3 \\ \dot{R}_2 \\ \dot{R}_3 \end{bmatrix} = \begin{bmatrix} -R_1 \cos \eta_1 \\ R_4 - R_1 \sin \eta_1 \\ R_1 \dot{\eta}_1 \sin \eta_1 \\ -R_1 \dot{\eta}_1 \cos \eta_1 \end{bmatrix}$$

Equation 56

Equation 56 can then be solved as:

$$\begin{bmatrix} R_2 \\ R_3 \\ \dot{R}_2 \\ \dot{R}_3 \end{bmatrix} = \begin{bmatrix} \frac{R_1 \sin(\eta_1 - \eta_3) - R_4 \cos \eta_3}{\cos(\eta_1 - \eta_3)} \\ \frac{R_1 - R_4 \sin \eta_1}{\cos(\eta_1 - \eta_3)} \\ \frac{2\dot{\eta}_1 R_1 - \dot{\eta}_1 R_4 \sin \eta_1 - \dot{\eta}_1 R_4 \sin(\eta_1 - 2\eta_3)}{\cos(2\eta_1 - 2\eta_3) + 1} \\ \frac{2\dot{\eta}_1 R_1 \sin(\eta_1 - \eta_3) - 2\dot{\eta}_1 R_4 \cos \eta_3}{\cos(2\eta_1 - 2\eta_3) + 1} \end{bmatrix}$$

Equation 57

Equation 57 thus allows the calculation of the instantaneous measurement position of the laser beam on the MBLEC (R_2) along with its instantaneous scanning speed \dot{R}_2 as functions of the laser beam orientation (defined by \bar{R}_3 and \bar{R}_4) as well as the rotation angle η_1 .

A.2.2 Rigid Body Velocity Component

Inherent to the RC ELDV measurement approach, is the presence of a Rigid Body Velocity Component (RBVC) in the measurements due to the circumferential velocity of the blade. To study this effect, vector-loop calculations are employed yet again. A new vector, \bar{R}_5 is defined stretching from the rotation centre to the end of \bar{R}_2 as seen in Figure 77:

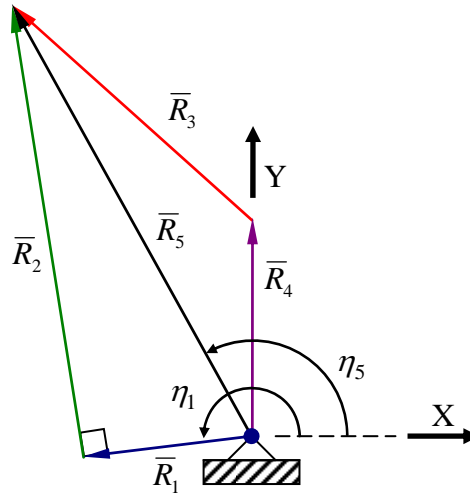


Figure 77: Vector-loop diagram for RBVC calculations

Using the vector-loop, the following relationships are obtained:

$$\bar{R}_5 = \bar{R}_1 + \bar{R}_2 = \bar{R}_3 + \bar{R}_4$$

Equation 58

Solving for the X-components yield :

$$\begin{aligned} R_5 \cos \eta_5 &= R_3 \cos \eta_3 \\ \cos \eta_5 &= \frac{R_3}{R_5} \cos \eta_3 \end{aligned}$$

Equation 59

while solving for the Y-components give:

$$\begin{aligned} R_5 \sin \eta_5 &= R_3 \sin \eta_3 + R_4 \\ \sin \eta_5 &= \frac{R_3}{R_5} \sin \eta_3 + \frac{R_4}{R_5} \end{aligned}$$

Equation 60

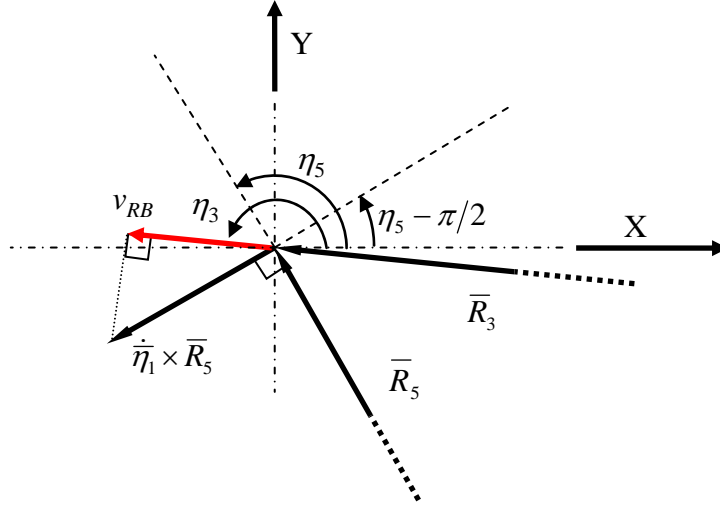


Figure 78: RBVC vector definition

Referring to Figure 78, v_{RB} can be calculated as follows:

$$\begin{aligned}
 v_{RB} &= \dot{\eta}_1 R_5 \cos(\eta_5 - 90^\circ + 180^\circ - \eta_3) \\
 &= \dot{\eta}_1 R_5 \cos(\eta_5 - \eta_3 + 90^\circ) \\
 &= \dot{\eta}_1 R_5 \sin(\eta_3 - \eta_5) \\
 &= \dot{\eta}_1 R_5 (\sin \eta_3 \cos \eta_5 - \cos \eta_3 \sin \eta_5)
 \end{aligned}$$

Equation 61

Substituting Equation 59 and Equation 60 into Equation 61:

$$\begin{aligned}
 v_{RB} &= \dot{\eta}_1 R_5 \left(\sin \eta_3 \frac{R_3}{R_5} \cos \eta_3 - \cos \eta_3 \frac{R_3}{R_5} \sin \eta_3 - \cos \eta_3 \frac{R_4}{R_5} \right) \\
 &= -\dot{\eta}_1 R_4 \cos \eta_3
 \end{aligned}$$

Equation 62

Since $\dot{\eta}_1 = 2\pi\psi$ is the rotor speed, v_{RB} can be expressed as:

$$v_{RB} = -2\pi\psi \cdot R_4 \cos \eta_3$$

Equation 63

From Equation 63 it can be deduced that if ψ is constant and the laser beam orientation is fixed, v_{RB} will be constant and will be manifested in the measurements as a DC offset.

A.2.3 The influence of BLEP variance from the MBLEC

The variance of the actual BLEP from the MBLEC will affect the actual instantaneous measurement position as shown in Figure 79, and as a result the scanning speed as well. Also the incidence angle of the laser beam on the surface normal will be affected by the curvature of the BLEP and may thus affect the range of η_1 for which useful measurements can be recorded.

Since v_{RB} is independent of measurement position, it remains unaffected by any variance of the BLEP from the MBLEC.

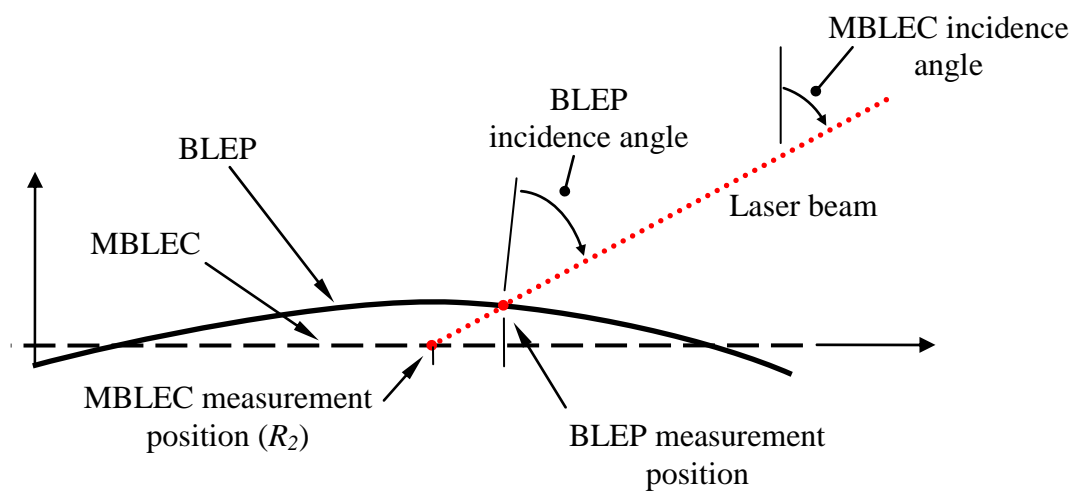


Figure 79: Effect of BLEP variance from MBLEC

A.3 Experimental verification



Figure 80: RC ELDV experimental setup

To verify the equations presented in Section A.2.2, experimental measurements were recorded on the single-blade rotor of Chapter 3. The experimental setup is demonstrated in Figure 80. To obtain the LDV orientation parameters, a tilt sensor was used to measure η_3 as well as the two values of η_2 for which $R_2 = 0.180$ m (i.e. when the blade tip enters and exits the laser beam). These two angles are labelled $\eta_{2,1}$ and $\eta_{2,2}$ respectively as shown in Figure 81. Since \bar{R}_1 and \bar{R}_2 are perpendicular, $\eta_{1,1}$ and $\eta_{1,2}$ is thus also known at these two positions. R_4 can then be obtained by rearranging the solution for R_2 of Equation 57 as shown in Equation 64 for $\eta_{1,1}$:

$$R_{4,1} = \frac{R_1 \sin(\eta_{1,1} - \eta_3) - R_2 \cos(\eta_{1,1} - \eta_3)}{\cos \eta_3}$$

Equation 64

Setting Equation 64 into Equation 63, v_{RB} can be expressed in terms of m/s/RPM as given for $\eta_{1,1}$:

$$v_{RB,1} = -(2\pi/60) \cdot [R_1 \sin(\eta_{1,1} - \eta_3) - R_2 \cos(\eta_{1,1} - \eta_3)]$$

Equation 65

The LDV orientation measurements and calculations are summarized in Table 10. Ideally $v_{RB,1}$ and $v_{RB,2}$ should be equal. However due to the resolution of the tilt sensor, $\eta_{2,1}$ and $\eta_{2,2}$ was measured with limited accuracy.

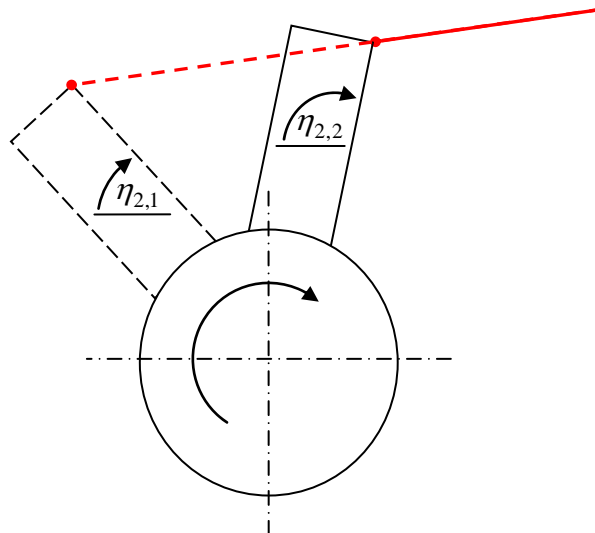


Figure 81: Experimental LDV orientation measurement

Table 10: LDV orientation measurements and calculations

	η_3	[°]	179.0
Position 1	$\eta_{2,1}$	[°]	32.7
	$\eta_{1,1}$	[°]	122.7
	$R_{4,1}$	[m]	0.110
	$v_{RB,1}$	[mm/s/RPM]	11.54
Position 2	$\eta_{2,2}$	[°]	139.1
	$\eta_{1,2}$	[°]	229.1
	$R_{4,2}$	[m]	0.106
	$v_{RB,2}$	[mm/s/RPM]	11.10

RC ELDV measurements were recorded on the blade during rotor run-up to 960 RPM as shown in Figure 82. From this figure a lower limit DC drift can be observed in the measurements. Although the lower limit of the measurements should be at 0 m/s (as seen at the start of the measurement), the LDV measurements start to drift at the lower rotor speeds and settles after about 13 s. This phenomenon is ascribed to the LDV measurement system. Feedback from the OEM was however not available.

To compare the measured and theoretical RBVCs, the experimental measurement range for each blade passage needs to be considered. The results are shown in Figure 83 and errors of 8.9 % and 4.7 % are observed for $v_{RB,1}$ and $v_{RB,2}$ respectively. Via optimization, $v_{RB,opt}$ was obtained as 10.60 mm/s/RPM which indicates angle measurement errors in $\eta_{2,1}$, $\eta_{2,2}$ and η_3 of about 1°. This corresponds to the errors that were measured during verification of the sensor.

From Figure 83, it is seen that a very good correlation exists between the experimental values of v_{RB} and $v_{RB,opt}$ although there is some difference at the lower rotor speeds. This discrepancy however occurs during the non-stationary phase of the measurement lower limit DC drift and is therefore probably a manifestation thereof.

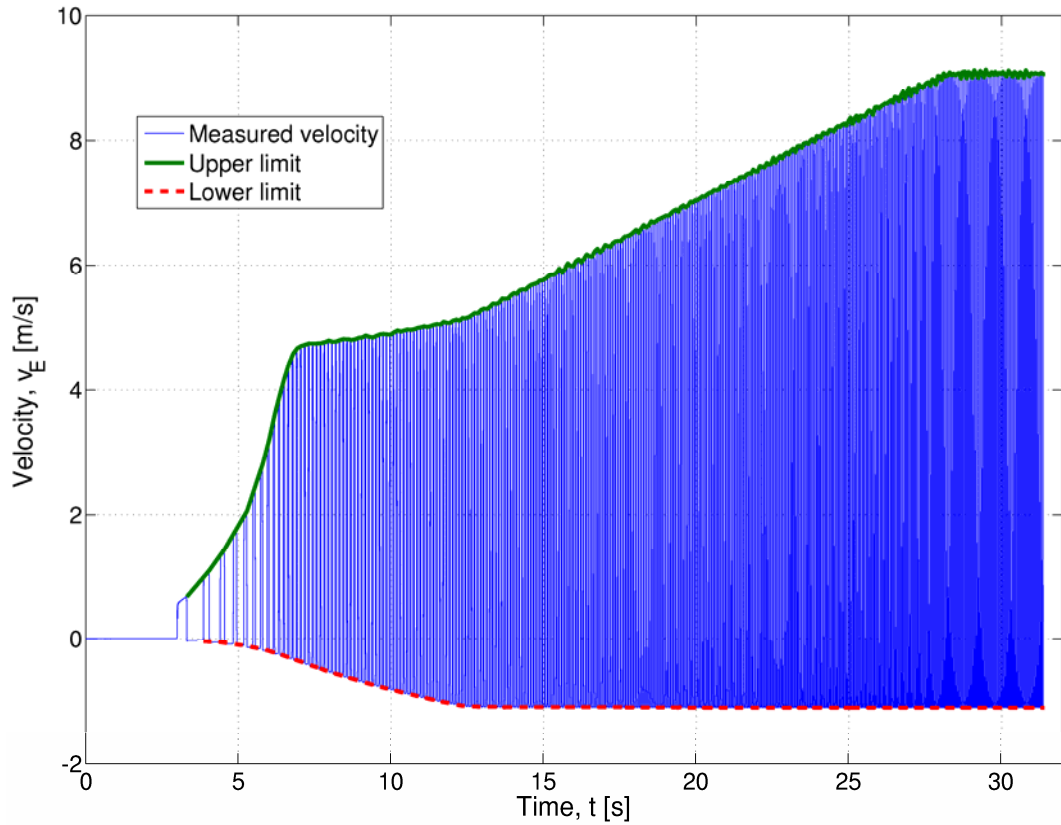


Figure 82: LDV drift

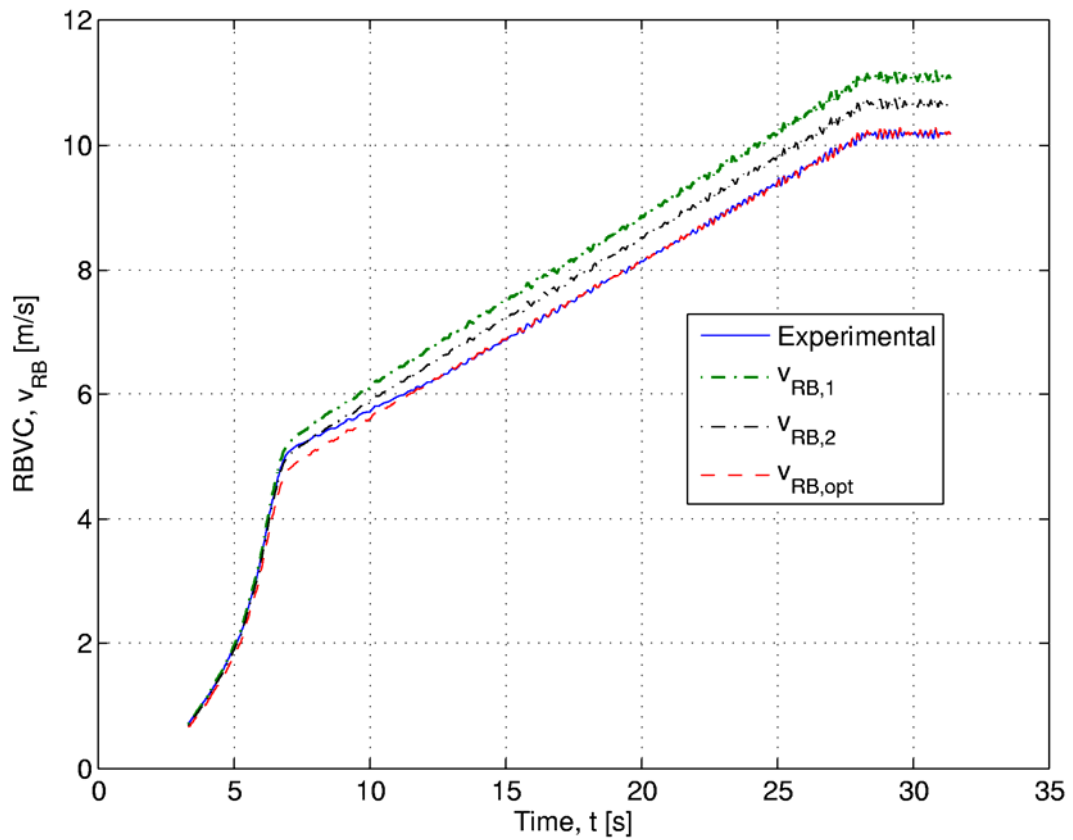


Figure 83: Comparison of measured and theoretical RBVCs

A.4 Response matrix interpolation for non-constant scanning speeds

In Equation 57, it was shown that the scanning speed along the blade edge during a single blade passage not constant:

$$c = \dot{R}_2 = \frac{2\dot{\eta}_1 R_1 - \dot{\eta}_1 R_4 \sin \eta_1 - \dot{\eta}_1 R_4 \sin(\eta_1 - 2\eta_3)}{\cos(2\eta_1 - 2\eta_3) + 1}$$

Equation 66

In Section 2.2.3 it was shown that LVRM interpolation can be successfully employed for constant scanning speeds. To perform this for a non-constant c , one approach is to construct the LVRM with a scan speed ratio $k=1$ (i.e. $c_{ref} = c = \dot{R}_2$). Another approach is to construct the LVRM for a constant c_{ref} chosen to obtain the required interpolation tolerance.

A.5 Conclusions

In this section, the peculiarities of the RC ELDV measurement approach were studied analytically using the vector-loop method. It was shown that RC ELDV introduces to the measurements a DC offset or RBVC which is directly proportional to the rotor speed. This was verified experimentally.

Observed in the experimental measurements was a lower limit DC drift, which is contributed to the SLDV system. Further work is thus necessary to establish the feasibility of this measurement approach.

The work of this section is presented in the article titled “*On the measurement of circumferential vibration on rotating blades using laser Doppler vibrometry*” (Oberholster and Heyns, In progress).